Applied Physics Research; Vol. 8, No. 4; 2016
ISSN 1916-9639 E-ISSN 1916-9647
Published by Canadian Center of Science and Education

A New Kinetics Defect Diffusion Model and the Critical Current Density of Semiconductor Laser Degradation

Jack Jia-Sheng Huang[1,2] & Yu-Heng Jan[2,1]

[1]Source Photonics, 8521 Fallbrook Avenue, Suite 200, West Hills, CA 91304, USA

[2] Source Photonics, No.46, Park Avenue 2nd Rd., Science-Based Industrial Park, Hsinchu, Taiwan, R.O.C.

Correspondence: Jack Jia-Sheng Huang, Source Photonics, 8521 Fallbrook Avenue, Suite 200, West Hills, CA 91304, USA. Tel: 818-266-7276. E-mail: jack.huang@sourcephotonics.com

Received: May 30, 2016 Accepted: June 12, 2016 Online Published: July 6, 2016

doi:10.5539/apr.v8n4p11 URL: http://dx.doi.org/10.5539/apr.v8n4p11

Abstract

Critical current density on the electromigration failure is a commonly observed phenomenon in the integrated circuit (IC) interconnect. The critical current density is important for the lognormal distribution and failure time extrapolation of IC metal conductors. In this paper, we report the critical current density (j_c) of semiconductor laser degradation for the first time. Despite of the different physical origin, the j_c of the laser degradation exhibits similar effect on the failure time distribution. We develop a new kinetic defect diffusion model that can account for the existence of j_c. We discuss the physical mechanism and its implication in the reliability extrapolation of diode lasers.

Keywords: semiconductor laser, reliability model, diffusion kinetics, critical current density, electromigration, IC interconnect

1. Introduction

Owing to the popularity of Facebook, Amazon, Netflix and Google, high-speed optical networks for datacenter, wireless and cloud computing are becoming increasingly popular. The hand-held mobile devices such as iPhone and iPad have further fueled the demand for ever-increasing internet speed and mega datacenter capacity. In order to enable social networking, web search and online purchasing, high-speed broadband transceivers have become the important building blocks in the modern communication network deployment (Basal, 2016; Bilal et al., 2013).

Reliability of diode laser is one of the most critical aspects to meet the environmental-friendly, energy-efficient and low-cost datacenters (Huang, 2015). One impact of reliability degradation is the higher power consumption related to increased bias current. The other is the waste of energy and cost to replace the failure parts. After a few decades of reliability studies on diode lasers, the optoelectronics industry has attained better understanding of degradation characteristics such as degradation behavior, failure criterion and temperature acceleration factor (Fukuda, 1988; Chin et al., 2003; Johnson, 2003; Sim, 1989; Huang, 2005; Huang et al., 2005; Lam et al., 2003; Chuang et al., 1998). On the other hand, there are still several outstanding reliability questions that remain challenging and debatable. The purpose of this study is to explore those unanswered fundamental questions that are important for product design and overall system robustness.

The first question concerns the burn-in behavior associated with rapid increase in the threshold current (I_{th}) during the first burn-in cycle, followed by a very small change in I_{th} during the second burn-in cycle. Engineers and scientisits often debate about whether the lasers are acceptable for production due to the concern of the large initial I_{th} changes. Some suggest to accept the diode lasers based on the nature of stable second burn-in, while others express concern about the large initial I_{th} increases. The physical mechanism has been largely unclear thus far. There was no model or theory developed in the past to explain why the lasers exhibited the large I_{th} increases, and suddenly became stable afterwards.

The second question is about the degradation behavior at low stress current regime. The laser diodes often exhibit little I_{th} changes when subjected to low stress conditions. Furthermore, the degradation at the low stress condition is usually slower than expected. One could observe a precipitously reduced degradation rate when the

stress current is decreased to a certain level. There was no previous model established to account for such dramatic change in the degradation behavior for the low stress current.

The third question pertains the failure time distributions of the lasers subjected to the low stress current aging. Typically, the failure times for the low stress current are longer than those for the high stress current. At the meantime, the sigma of the failure times for the low stress current also tends to increase. The large sigma or dispersion in the failure distribution often results in a net increase in the failure rate, which makes the interpreation of reliability more complex. It has been unclear why the failure distributions of the lasers for the low stress current deviate from the normal stress current. For the latter, the failure distribution shows lognormal distribution. For the former, the failure distribution shows strong modification from lognormal.

2. Historical Background: Critical Current Density of IC Interconnect Electromigration

Electromigration is one of the key factors responsible for long-term interconnect wear-out. Under the high electric field, there is an electron wind force that imposes on the metal atoms to result in a net mass transport. When electromigration occurs, there is void formation at the cathode and extrusion at the anode (Ho et al., 1989; Tu et al., 1992). The electrical characteristics of electromigration degradation is typically associated with resistance increase (Huang et al., 2001; Hu et al., 1995). Failure time of interconnect is commonly defined as the time to reach 20% increase in resistance (ΔR=20%).

Forty years ago in 1976, Blech and Herring reported a critical current density of electromigration (Blech, 1976; Blech et al., 1976). It was found that no electromigration occurred below a certain length due to the back stress generated in the metal stripe. For modern IC interconnect, the characterization of the critical current density for electromigration is important for reliability model development. The effect of critical current density on electromigration has been experimentally observed in Al, Al(Cu) and Cu dual-damascene vias (Thompson et al., 1993; Proost et al., 2000; Huang et al., 2000; Lee et al., 1995). Researchers have also shown the influence of j_c on the failure time distributions. Oates (Oates, 1996) and Huang (Huang et al., 2000) showed the deviations of failure distribution in the Al(Cu) interconnects as j approached j_c. Recently, Oates et al. (Oates et al., 2009) demonstrated similar modification of failure time distributions from lognormal in the Cu dual-damascene as the current densities approached j_c.

3. Experimental

Figures 1(a) and (b) shows the cross-sectional schematics of the ridge waveguide (RWG) and buried heterostructure (BH) laser structures, respectively. Both structures were grown by the metal organic chemical vapor deposition (MOCVD) technique. The single-mode distributed feedback (DFB) was defined by holographic grating. For the RWG structure in Figure 1a, one step regrowth after grating was performed to form the p-InP cladding and p^+-InGaAs contact. The active region consisted of InGaAlAs multi-quantum well (MQW) materials. For the BH structure in Figure 1b, three regrowth steps including grating overgrowth, blocking regrowth and final regrowth were performed to complete the epitaxial layers. The first regrowth was performed after the grating etch; the second regrowth was performed after the mesa etch to form the active region; the final regrowth consisted of the p-InP cladding and p^+-InGaAs contact.

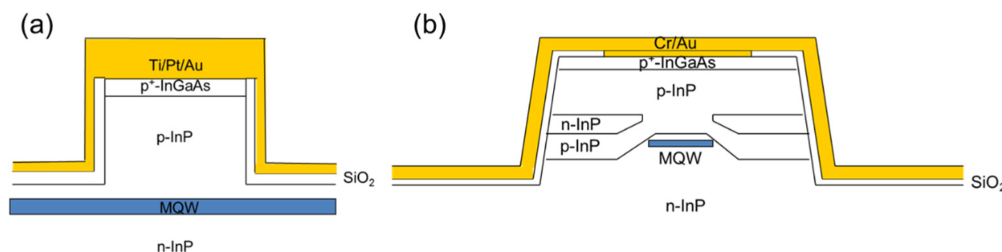

Figure 1. Schematics of the fabricated (a) ridge waveguide and (b) buried heterostructure lasers.

After the MOCVD regrowth, the wafers were processed with multiple lithography steps. The first lithography involved the ridge definition using the hard mask. The ridge structures (for both RWG and BH) were covered with the SiO_2 passivation for electrical isolation. The SiO_2 dielectric layer was then etched before the deposition of p-metal of Ti/Pt/Au to make ohmic contact. The wafer backside was thinned and deposited with n-metal of AuGe/TiAu.

To study the reliability, the laser diodes were stressed with different levels of currents to establish statistical data. The light versus current (LI) was tested before and after each reliability test interval. Due to the sample availability, RWG lasers of 1270nm lasing wavelength and BH lasers of 1550nm were used for the reliability study in this paper.

4. Results and Discussions

4.1 Kinetics model of defect diffusion

The laser degradation was related to defect formation (Endo et al., 1982; Fukuda, 1991; Hutchinson et al., 1975; Huang, 2012; Kallstenius, 1999). To study the degradation behavior, it is critical to understand the evolution of defect density during the aging process. Our previous model (Huang et al., 2016) assumed that the defect was formed at the surface damaged region and the defect diffusion involved propagation towards the active region. The defect concentration followed the Gauss error function where the surface concentration was the highest at the surface and decreased along the propagation direction.

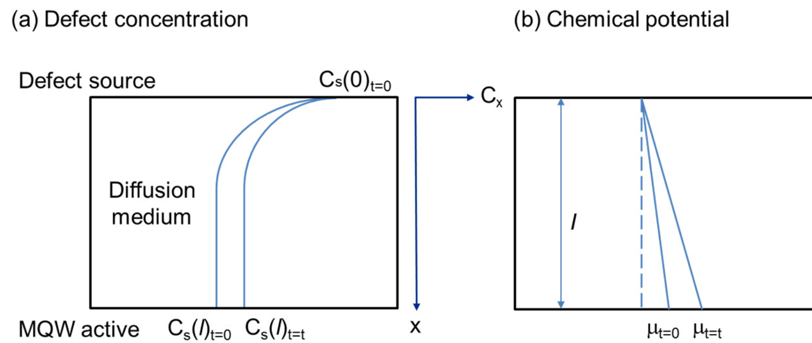

Figure 2. (a) Defect concentration and (b) chemcial potential at the active region before (time=0) and after aging (time=t). The defect souce could originate from the p-contact, BH interface or substrate dislocation network

In this paper, we expand the model to account for the kinetics of the defect diffusion process in general case, as illustrated in Figure 2a. First, the model assumes that the laser degradation is related to the diffusion from the defect source to the MQW active region. The defect source could be from the p-contact (Huang, 2012; Huang et al., 2016), the BH interface (Fukuda et al., 1987; Mawatari et al., 1997) or the substrate dislocation network (Petroff et al., 1976; O'Hara et al., 1977). Second, the model includes the kinetics of defect diffusion that is driven by the electric current and field. The flux of the defect from the source into the active region can be expressed as

$$J = C\frac{D}{kT}(Q^* E) \qquad \text{Equation (1)}$$

where C is the atomic defect concentration, D is the diffusivity of the defect, k is the Boltzmann constant, T is the temperature, Q* is the effective defect charge and E is the electric field. From electromagnetics theory, the electric field can be related to the current density (Reitz et al., 1979). Thus, Equation (1) can be rewritten as

$$J = C\frac{D}{kT}Q^* \rho j \qquad \text{Equation (2)}$$

where ρ is the resistivity and j is the current density.

In the next step, we attempt to develop the mathematical model to account for the experimental observation that the degradation tends to become slower over time. Assuming that the distance from the defect source to the active region is l, the defect concentration at the source and the active region are denoted as $C_s(0)$ and $C_s(l)$, respectively. In the beginning (t=0), the defect concentration $C_s(l)_{t=0}$ follows the Gauss error curve. After the initial aging at time of t, the threshold current is increased, so the defect concentration at the active region can be expressed as

$$C_s(l)_{t=t} = C_s(l)_{t=0}\left(\frac{I_{th}(t)}{I_{th}(0)}\right) \qquad \text{Equation (3)}$$

When the defect concentration builds up at the active region, the chemical potential of the defect increases, as illustrated in Figure 2b. The chemical potential is defined by the thermodynamics terms as the increase in the Gibbs free energy of the system per mole (Gaskell, 1981). We speculate that there is a force of “backflow” due to the chemical potential, similar to the back stress effect in the case of electromigration. The backflow can be formulated by the second term in Equation (4)

$$J = C\frac{D}{kT}(Q^*\rho j - \frac{\partial \mu}{\partial x}) \quad \text{Equation (4)}$$

where is the chemical potential of the defect, x is the axis along the defect propagation direction. When the backflow and the electrical force reach the equilibrium, the two forces cancel each other. At the equilibrium state, there is no net flux of defect diffusion. Hence, the I_{th} value remains the same with no more increase.

$$Q^*\rho j_c = \frac{\Delta\mu}{l} \quad \text{Equation (5)}$$

where j_c is the critical current density where no laser degradation occurs, and $\Delta\mu$ is the maximum chemical potential hat the defect can build up locally. The flux of defect can be rewritten in terms of critical current density

$$J = C\frac{D}{kT}Q^*\rho(j - j_c) \quad \text{Equation (6)}$$

The flux of defect can be simplified as the drift velocity according to the relation of v_d=J/C.

$$v_d = \frac{D}{kT}Q^*\rho(j - j_c) \quad \text{Equation (7)}$$

The failure time is proportional to the time to accumulate enough defects in the active region to cause the failure. The failure time can be expressed as

$$t_f = \frac{V_c}{Av_d} \quad \text{Equation (8)}$$

where V_c is the volume of defect needed to cause failure, and A is the cross-sectional area of the laser stripe.

$$t_f = \frac{(V_c / A)kT}{DQ^*\rho(j - j_c)} \quad \text{Equation (9)}$$

Since the width of the active region is typically pre-determined by the process to match the performance design target, the current density for the laser diode is specified as the current density (j) times the active width (w) or the applied bias current (I) divided by the cavity length (L).

$$t_f = \frac{(V_c / L)kT}{DQ^*\rho(j - j_c)w} \quad \text{Equation (10)}$$

4.2 Experimental Data

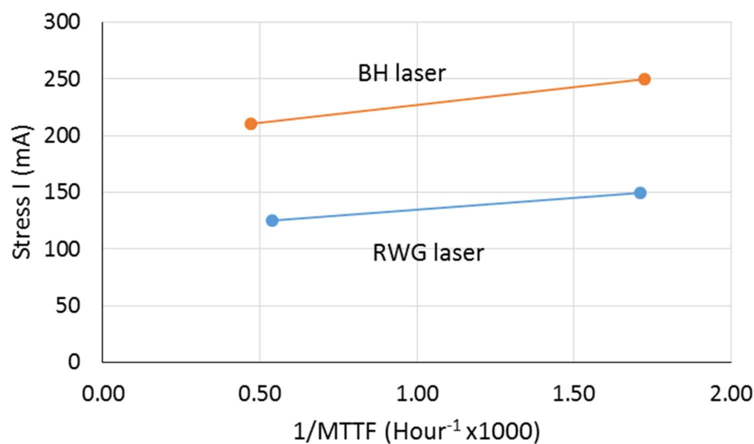

Figure 3. The plot of stress current versus reciprocal of failure time

For the semiconductor lasers, the stress current is typically specified based on the device operating condition. Hence, the stress bias is usually specified by the current as well. For example, the uncooled lasers typically operate at low bias around 30-60mA (Klotzkin et al., 2007; X. Ge et al., 2012; Lu et al., 2008), the analog cooled lasers tend to operate around 60-100mA (Huang et al., 2014), while the high power lasers typically operate at high bias around 350-600mA (Huang et al., 2008; Huang et al., 2012). Figure 3 shows the stress current plotted against the reciprocal of mean time-to-failure (MTTF). The MTTF is taken from the median value of the failure time distributions. For this study, the RWG lasers of 300μm were stressed with the current of 125-150mA, and the BH lasers of 550μm were stressed with 210-250mA. The stress current for the BH was higher than that of the RWG to accommodate the longer cavity length.

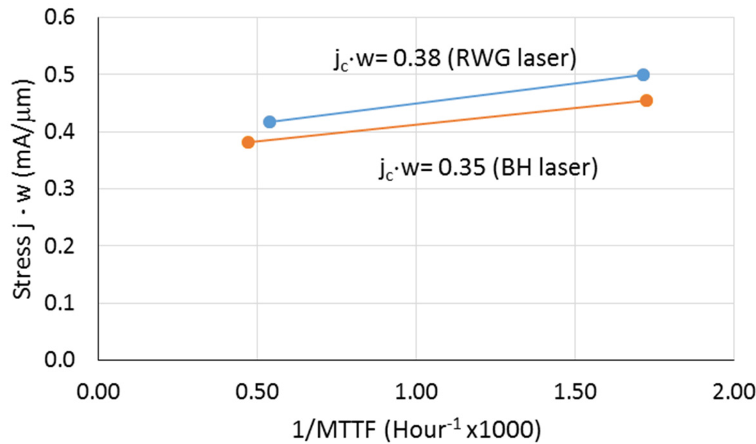

Figure 4. The plot of stress current density times active width versus reciprocal of failure time. The j_c is extracted from the intercept where 1/MTTF equals to 0

Next, we examine the relationship of stress current density times the active width (j·w) versus the reciprocal of MTTF to compare it with the model in Equation (10). By rearrangement of the variables, Equation (10) can be rewritten as Equations (11) and (12) where j·w is in the vertical axis and 1/MTTF is in the horizontal axis. Figure 4 shows the j·w plotted against 1/MTTF to determine the intercept. Several interesting features were observed. First, the MTTF between the RWG and BH was close to each other when normalized to the stress current density. Secondly, there existed a "critical current density" from the experimental data. Finally, the critical current density j_c·w, extracted from the intercept where 1/MTTF equaled to zero, was similar between the RWG and BH lasers. The values of j_c·w for RWG and BH lasers were determined to be 0.38 and 0.35mA/μm, respectively. Using the active width of 1.8μm, the corresponding j_c values for RWG and BH were 0.21 and 0.19mA/μm^2, respectively.

$$(j - j_c)w = \frac{(V_c / L)kT}{DQ^* \rho}\left(\frac{1}{t_f}\right) \quad \text{Equation (11)}$$

$$jw = j_c w + \frac{(V_c / L)kT}{DQ^* \rho}\left(\frac{1}{t_f}\right) \quad \text{Equation (12)}$$

The existence of j_c implies that there is a stress current density threshold below which no degradation would occur. In the following, we attempt to explain the fundamental unanswered questions about the observed degradation phenomena mentioned in the Introduction section.

The first myth concerned the burn-in behavior associated with rapid increase in the threshold current (I_{th}) during the first burn-in cycle, followed by a very small change in I_{th} during the subsequent burn-in cycles (see Type-A in Figure 5). The subsequent smaller changes can be attributed to the backflow effect. After the large initial I_{th} increase occurred, the defect concentration at the active region increased. As a result, the chemical potential gradient (∂μ/∂x) that could oppose the diffusion from the defect source became higher. According to Equation (4), the net flux or drift velocity of the defect diffusion became lower. In constrast, some lasers exhibited smaller initial I_{th} increase followed by gradual I_{th} stabilization during the subsequent burn-in, as illustrated in Type-B in Figure 5. The smaller I_{th} increase led to lower chemical potential that would allow continued defect diffusion due to the net flux. The I_{th} increase would follow gradual pattern until the chemical potential (the second term in Equation 4) eventually became large enough to offset the electric current force (the first term in Equation 4).

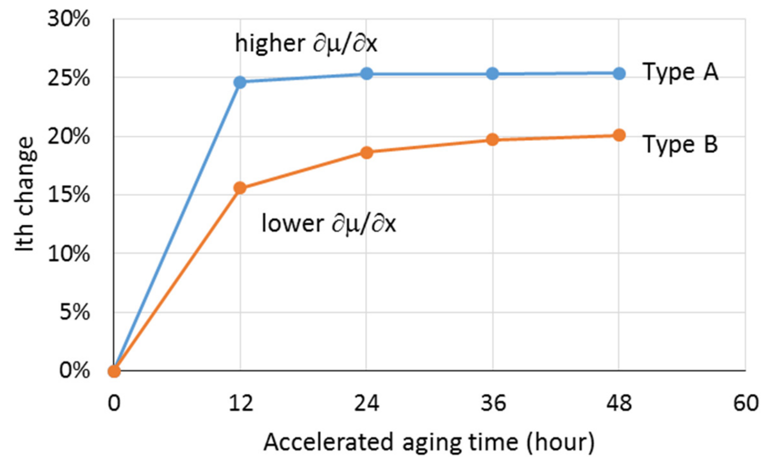

Figure 5. The relative I_{th} change as a function of accelerated aging time for Type-A and Type-B. Type-A is characterized with larger initial I_{th} increase followed by full stabilization. Type-B is featured with smaller initial I_{th} increase followed by gradual stabilization

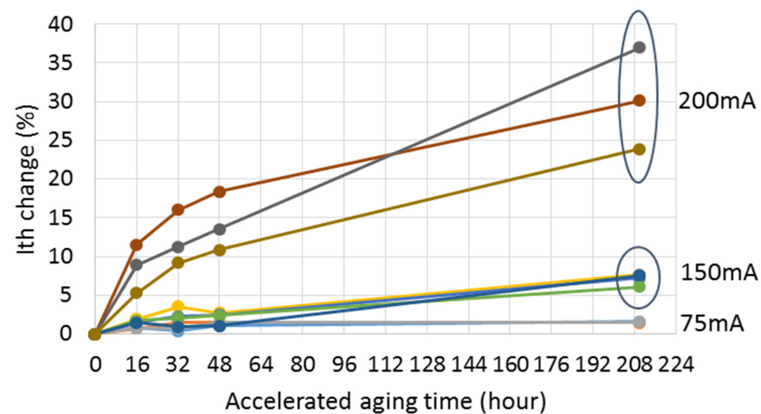

Figure 6. The relative I_{th} change of laser devices as a function of stress current. For the low stress current (75mA), the degradation was very little due to small $j-j_c$. For the medium stress current (150mA), the degradation was observable as j moved away from j_c. For the high stress current (200mA), the degradation became pronounced due to large $j-j_c$

The second myth was about the degradation behavior at low stress current regime. The laser diodes often exhibited little I_{th} changes when subjected to low stress conditions. Furthermore, the degradation at the low stress condition was usually slower than expected. According to Equation 11, 1/MTTF became infinitely small as j approached j_c. In other word, the MTTF became infinitely high as j approached j_c. The effect of j_c could account for the experimentally observed slow degradation for the low stress regime. Figure 6 illustrates the effect of $(j-j_c)$ from the same type of devices that were subjected to different levels of stress currents. For the low stress current (75mA in this case), the degradation curve was very small due to the small value of $j-j_c$. When extrapolated to the end-of-lifetime, the failure time would be very large that would lead to a very small value of 1/MTTF. For the medium stress current (150mA), the degradation curves were more observable as j moved away from j_c. The reliability data based on the medium stress current regime was typically suitable for the determination of j_c. For the high stress current (200mA), the degradation was pronounced due to the large j with reference to j_c. In this regime, the degradation rate was likely larger than expected due to Joule heating. Care needed to be taken when using the degradation data of the high stress current regime to estimate the device lifetime.

The third myth pertained the failure time distributions of the lasers subjected to the low stress current aging. As shown in Figure 7, the failure times for the low stress current were typically longer than those for the high stress current. At the meantime, the sigma of the failure times for the low stress current also tended to increase. The deviation of the low failure distribution of the low stress regime from lognormal could be attributed to the effect of j_c. According to Equation 10, t_f was inversely proportional to $j-j_c$. The Monte-Carlo simulation would result in

the strong modification of failure distributions as j approaches j_c (Huang & Oates, 2000). This was likely due to the smaller value of (j-j_c) in the denominator.

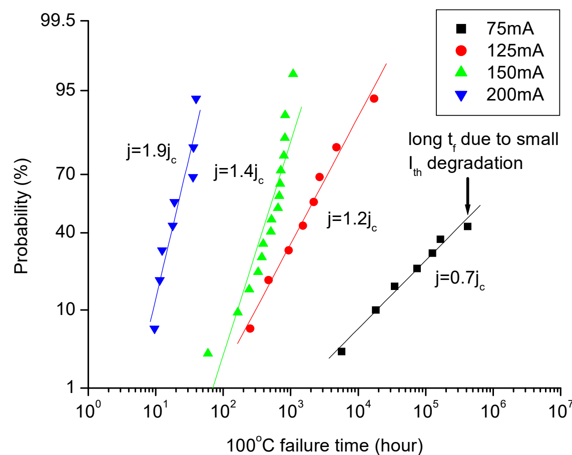

Figure 7. Failure time distributions of laser devices that were subjected to different stress current density with respect to j_c. The symbols are taken from experimental data, and the lines are from regression fitting

5. Conclusion

We developed the new kinetics model of defect diffusion processes for the RWG and BH semiconductor lasers. The model was based on the kinetics process of the defect diffusion from the source to the active region. The defect source could be from the p-contact, BH interface or substrate dislocation. The model introduced the chemical potential of the defect at the active as the “backflow” force to oppose the defect diffusion driven by the electric current. The model suggested that there existed a critical current density (j_c) below which no degradation would occur. The j_c represented the back flow effect due to the chemical potential of the defect at the active region. Experimental data showed that $j_c \cdot w$ was close to 0.36mA/µm, corresponding to the j_c estimation value of 0.20mA/µm^2.

The effect of j_c seemed to provide good explanation for several unanswered questions: (1) The larger the initial I_{th} increase was, the smaller the subsequent I_{th} change would occur due to the higher chemical potential of the defect at the active region. (2) The degradation was usually slower than expected for the low stress current due to the “backflow” effect of j_c. (3) The deviation of failure distribution from lognormal for the low stress current due to the effect of j_c. Despite of the different physical origin, the j_c of the laser degradation exhibited similar effect on the failure time distribution compared to electromigration in the IC interconnect.

Acknowledgment

The authors would like to thank Jesse Chang for the assistance in test data collection, Emin Chou for support of this work and wafer fab team in Source Photonics, Taiwan for chip processing and testing.

References:

Basal, J. (2016). Source Photonics announces shipment of 10,000 single mode 100G QSFP28 modules. *Optical Fiber Communications Conference* (OFC, Anaheim, CA).

Bilal, K., Khan, S. U., & Zomaya, A. Y. (2013). Green Data Center Networks: Challenges and Opportunities. In 11th *IEEE International Conference on Frontiers of Information Technology (FIT*), Islamabad, Pakistan, 229-234. http://dx.doi.org/10.1109/fit.2013.49

Blech, I. A. (1976). Electromigration in thin aluminum films on titanium nitride, *J. Appl. Phys., 47*(4), 1203-1208. http://dx.doi.org/10.1063/1.322842

Blech, I. A., & Herring, C. (1976). Stress generation by electromigration, *Appl. Phys. Lett., 29*(3), 131-133. http://dx.doi.org/10.1063/1.89024

Chin, A. K., Zipfel, C. L., Geva, M., Gamlibel, I., Skeath, D., & Chin, B. K. (1984). Direct evidence for the role of gold migration in the formation of dark-spot defects in 1.3µm InP/InGaAsP light emitting diodes. *Appl. Phys. Lett., 45*(1), 37–39. http://dx.doi.org/10.1063/1.94995

Chuang, S. L., Nakayama, N., Ishibashi, A., Taniguchi, S., & Nakano, K. (1998). Degradation of II-VI blue-green semiconductor lasers. *IEEE J. Quantum Electron., 34*(5), 851–857. http://dx.doi.org/10.1109/3.668773

Endo, K., Matsumoto, S., Kawano, H., Sakuma, I., & Kamejima, T. (1982). Rapid degradation of InGaAsP/InP double heterostructure lasers due to <110> dark line defect formation. *Appl. Phys. Lett., 40*(11), 921–923. http://dx.doi.org/10.1063/1.92979

Fukuda, M. (1988). Laser and LED reliability update. *J. Lightw. Technol., 6*(10), 1988, 1488–1495. http://dx.doi.org/10.1109/50.7906

Fukuda, M. (1991). *Reliability and Degradation of Semiconductor Lasers and LEDs* (Chapter 4). Norwood, MA, USA, Artech House.

Fukuda, M., Noguchi, Y., Motosugi, G., Nakano, Y., Tsuzuki, N., & Fujita, O. (1987). Suppression of interface degradation in InGaAsP/InP buried heterostructure lasers, *J. Lightw. Technol., LT-5*(12), 1778-1781. http://dx.doi.org/10.1109/JLT.1987.1075475

Gaskell, D. R. (1981). *Introduction to metallurgical thermodynamics* (Chapter 5). New York, NY, USA, McGraw-Hill.

Ge, X., Moat, P., Xie, J., Hu, J., Huang, J. S., Su, X., … Klotzkin, D. (2012). Thermal conductivity of 1.3μm InAs/GaAs quantum dot laser active material from chirp and 3ω measurements. *Appl. Phys Lett., 100*(8), 082108. http://dx.doi.org/10.1063/1.3687160

Ho, P. S., & Kwok, T. (1989). Electromigration in metals. *Rep. Prog. Phys., 52*, 301–348. http://dx.doi.org/10.1088/0034-4885/52/3/002

Hu, C. K., Luther, B., Kaufman, F. B., Hummel, J., Uzoh, C., & Person, D. J. (1995). Copper interconnection integration and reliability, *Thin Solid Films, 262*(1-2), 84-92. http://dx.doi.org/10.1016/0040-6090(94)05807-5

Huang, J. S. (2005). Temperature and current dependences of reliability degradation of buried heterostructure semiconductor lasers. *IEEE Trans. Device Mater. Reliab., 5*(1), 150-154. http://dx.doi.org/10.1109/TDMR.2005.843834

Huang, J. S. (2012). Design-in reliability for modern wavelength-division multiplex (WDM) distributed feedback (DFB) InP lasers. *Appl. Phys. Res., 4*(2), 15-28. http://dx.doi.org/10.5539/apr.v4n2p15

Huang, J. S. (2015). *Reliability of optoelectronics* (Chapter 6, J. Swingler (Ed.)). Cambridge, UK, Woodhead Publishing. http://dx.doi.org/10.1016/b978-1-78242-221-1.00006-x

Huang, J. S., Oates, A. S., Obeng, Y. S., & Brown, W. L. (2000). Asymmetrical critical current density and its influence on electromigration of two-level W-plug interconnection, *J. Electrochem. Soc., 147*(10), 3840-3844. http://dx.doi.org/10.1149/ 1.1393982

Huang, J. S., & Oates, A. S. (2000). Monte-Carlo simulation of electromigration failure distribution of submicron contacts and vias: a new extrapolation methodology for reliability estimate. *Proc. International Interconnect Technology Conference (IITC*), 208-210. http://dx.doi.org/10.1109/iitc.2000.854327

Huang, J. S., He, X., Blauvelt, H., Chin, H., Lomeli, M., & Zendejaz, R. (2014). Cost-effective O-band high-power, low distortion CWDM analog lasers, *IEEE Photonics Conference* (San Diego, CA, USA), 461-462.

Huang, J. S., Isip, E., & Carson, R. F. (2012). High-resolution wavelength stability aging study of C-band 100mW high-power DWDM laser modules, *IEEE Photonics Conference* (Burlingame, CA, USA), 538-539.

Huang, J. S., Jan, Y. H., Ren, D., Hsu, Y., Sung, P., & Chou, E. (2016). Defect diffusion model of InGaAs/InP semiconductor laser degradation, *Appl. Phys. Research, 8*(1), 149-157. http://dx.doi.org/10.5539/apr.v8n1p149

Huang, J. S., Nguyen, T., Hsin, W., Aeby, I., Ceballo, R., & Krogen, J. (2005). Reliability of Etched-Mesa Buried-Heterostructure Semiconductor Lasers. *IEEE Trans. Device Mater. Reliab., 5*(4), 665-674. http://dx.doi.org/10.1109/TDMR.2005.860562

Huang, J. S., Shofner, T. L., & Zhao, J. (2001). Direct observation of void morphology in step-like electromigration resistance behavior and its correlation with critical current density. *J. Appl. Phys., 89*(4), 2130-2133. http://dx.doi.org/10.1063/1.1340004

Huang, J.S., Lu, H., & Su, H. (2008). Ultra-high power, low RIN and narrow linewidth lasers for 1550nm DWDM 100km long-haul fiber optic link, *LEOS Conference* (Newport Beach, CA, USA), 894-895. http://dx.doi.org/10.1109/leos.2008.4688910

Hutchinson, P. W., & Dobson, P. S. (1975). Defect structure of degraded GaAlAs-GaAs double heterojunction lasers. *Phil. Mag., 32*, 745–754. http://dx.doi.org/10.1080/14786437508221617

Johnson, L. A. (2003). Reliability counts for laser diodes. *Photonics, 37*(7), 55-56.

Kallstenius, T., Bäckström, J., Smith, U., & Stoltz, B. (1999). On the degradation of InGaAsP/InP-based bulk lasers. *J. Lightw. Technol., 17*(12), 2584. http://dx.doi.org/10.1109/50.809681

Klotzkin, D., Huang, J. S., Lu, H., Nguyen, T., Pinnington, T., Rajasekarem, R., & Tsai, C. (2007). An optimized structure for InGaAlAs spot size converted lasers for direct fiber coupling fabricated without overgrowth, *IEEE Photonics Tech. Lett., 19*(13), 975-977. http://dx.doi.org/10.1109/LPT.2007.898824

Lam, S. K. K., Mallard, R. E., & Cassidy, D. T. (2003). Analytical model for saturable aging in semiconductor lasers. *J. Appl. Phys., 94*(3), 1803–1809. http://dx.doi.org/10.1063/1.1589594

Lee, K. L., Hu C. K., & Tu, K. N. (1995). *In-situ* scanning electron microscope comparison studies on electromigration of Cu and Cu(Sn) alloys for advanced chip interconnects, *J. Appl. Phys., 78*, 4428-4437. http://dx.doi.org/10.1063/1.359851

Lu, H., Huang, J. S., & Su, H. (2008). Ultra-high speed 1.3μm complex-coupled DFB lasers for future uncooled 10Gb/s GPON, *IEEE Int'l Semiconductor Laser Conference (ISLC)* (Sorrento, Italy), 15-16.

Mawatari, H., Fukuda, M., Matsumoto, S., Kishi, K., & Itaya, Y. (1997). Reliability and degradation behaviors of semi-insulating Fe-doped InP buried heterostructure lasers fabricated by RIE and MOVPE. *J. Lightw. Technol., 15*(3), 534-537. http://dx.doi.org/10.1109/50.557570

O'Hara, S., Hutchinson, P. W., & Dobson, P. S. (1977). The origin of dislocation climb during laser operations. *Appl. Phys. Lett., 30*(8), 368-371. http://dx.doi.org/10.1063/1.89432

Oates, A. S. & Lin, M. H. (2009). Electromigration failure distributions of Cu/low-k dual-damascene vias: impact of the critical current density and a new reliability extrapolation methodology. *IEEE Trans. Dev. Mater. Reliab., 9*(2), 244-254. http://dx.doi.org/10.1109/TDMR.2009.2015767

Oates, A. S. (1996). Electromigration failure of contacts and vias in sub-micron integrated circuit metallizations, *Microelectron. Reliab., 36*(7/8), 925-953. http://dx.doi.org/10.1016/0026-2714(96)00102-3

Petroff, P. M., & Kimerling, L. C. (1976). Dislocation climb model in compound semiconductors with zinc blende structure. *Appl. Phys. Lett., 29*(8), 461-463. http://dx.doi.org/10.1063/1.89145

Proost, J., Maex, K., & Delaey, L. (2000). Electromigration-induced drift in damascene and plasma-etched Al(Cu). II. Mass transport mechanisms in bamboo interconnects. *J. Appl. Phys., 87*, 99–109. http://dx.doi.org/10.1063/1.372389

Reitz, J. R., Milford, F. J., & Christy, R. W. (1979). *Foundations of electromagnetic theory*. Reading, MA, USA, Addison-Wesley Publishing.

Sim, S. P. (1989). A review of the reliability of III-V opto-electronic components, in *Proc. Semiconductor Device Reliability: Advanced Workshop II, NATO International Scientific Exchange Program*, Crete, Greece, 301.

Thompson, C. V., & Lloyd, J. R. (1993). Electromigration and IC interconnects, *MRS Bulletin,* 19-25.

Tu, K. N., Mayer, J. W., & Feldman, L. C. (1992). *Electronic thin film science for electrical engineers and materials scientists* (Chapter 14). New York, NY, McMillan Publishing.

Copyrights

Copyright for this article is retained by the author(s), with first publication rights granted to the journal.

This is an open-access article distributed under the terms and conditions of the Creative Commons Attribution license (http://creativecommons.org/licenses/by/3.0/).